Research Activities

– Off-line Experiments –

Temperature dependent study of the Dirac point energy gap in magnetic stoichiometric topological insulators $MnBi_2Te_4$

D. A. Estyunin[a], I.I. Klimovskikh[a], A.M. Shikin[a], A. Kimura[b], S. Kumar[c] and E.F. Schwier[c]

[a] *Saint Petersburg State University, Saint Petersburg, 198504 Russia*
[b] *Department of Physical Sciences, Graduate School of Science, Hiroshima University, Hiroshima, Japan*
[c] *Hiroshima Synchrotron Radiation Center, Hiroshima University, Hiroshima, Japan*

Keywords: Magnetic stoichiometric topological insulator, $MnBi_2Te_4$, the Dirac point band gap

In this report we will present continuation to the study of antiferromagnetic (AFM) topological insulator (TI) $MnBi_2Te_4$ (MBT) [1]. It is characterised by a high Néel temperature (T_N) and a large band gap at the Dirac point (DP) in comparison with magnetically doped TIs. The material has a layered structure and consists of septuple layer (SL) blocks [Te-Bi-Te-Mn-Te-Bi-Te] stacked along the *c* axis and separated by van

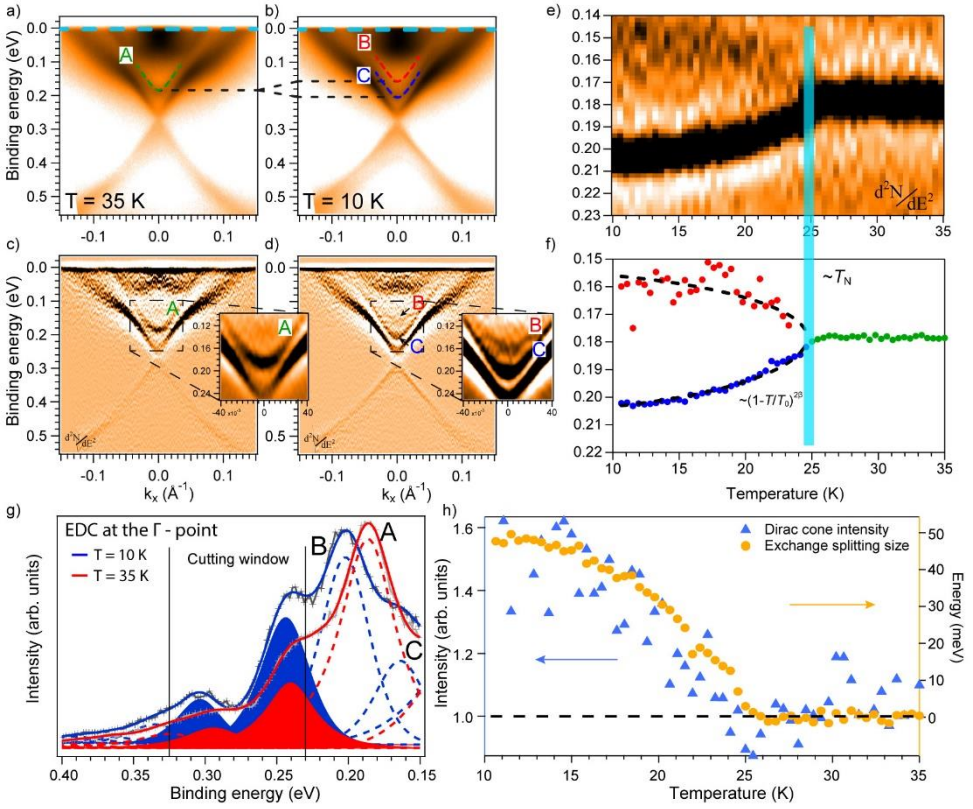

FIGURE 1. (a,b) Band dispersion $E(k_x)$ of AFM TI MBT measured along GK direction with photon energy of 6.3 eV at T = 35 K and T = 10 K, respectively. (c,d) the second derivatives of (a,b). Green, red and blue dashed curves with corresponding labels (A, B and C) in panels (a,b,c,d) show states of interest. (e) Temperature dependence of states (A),(B) and (C) at the Γ point (T = 10 K to 35 K, dT=0.5 K). (f) Dots show positions of peaks from fitting of corresponding profiles from (e). Black curves below 25 K are fitting experimental peaks positions with standard power law. (g) Spectral decomposition of the Γ-point energy distribution curves (blue – 10 K, red – 35 K), solid peaks are for the Dirac cone components. (h) Dirac cone intensity at the Γ point and spitting size plotted as function of temperature. Figures are taken from [4].

der Waals gaps. From magnetic measurements it was shown that MBT exhibits an A-type AFM ordering with an easy axis perpendicular to the layers, i.e. parallel to *c* [1,2]. According to theoretical calculations and direct magnetic measurements T_N of MBT is about 25 K [3]. Below T_N theory predicts an opening of a giant band gap of ~ 80 meV at the DP in case of A-type AFM ordering [1].

In Figs.1(a,b) we present MBT band structure well above and below T_N. One can identify a band marked by the green dashed line (A), which is clearly visible in the second derivative in panel (c). According to *ab initio* calculations [1], this state corresponds to the bottom of the BCB and has a weak dispersion along the k_z direction. Below T_N (b) the original single band (A) now visibly splits into two bands, marked with red and blue curves and labeled as (B) and (C). Despite its weak intensity the lower binding energy band (B) can be observed in the second derivative plot (Fig.1(d) and its inset).

In panel (e) an evolution of MBT electronic structure across the AFM/paramagnetic transition is shown (as the second derivative). One can clearly see that the band (A) splits into two (B) and (C) upon crossing T ≈ 25 K. We estimated energies of corresponding bands by fitting EDC profiles with one (T > 25 K) and two (T < 23 K) Voigt profile(s). The resulting binding energies are plotted in (f). At 10 K the states are well separated by ≈ 45 meV and move closer to their common center of mass with elevated temperatures, merging at 25 K.

Observed behavior of bands splitting is reminiscent to exchange splitting in magnetic compounds. Assuming this, we estimate the experimental energy splitting with use of the standard power law (see (e)). The results of the fitting well match the observed temperature dependence. Estimated onset temperature T_0 matches well with T_N [1]. These observations can prove influence of magnetism on electronic structure in MBT. Moreover, one can probe magnetic properties of MBT compounds simultaneously with electronic structure at the same position by estimating the splitting parameters (onset temperature and saturation splitting).

Finally, we analyze the response of topological surface states (TSS) to the magnetic ordering. While theory undoubtedly predicts an opening of a giant band gap up to 90 meV for A-type AFM ordering, experimental results have a wide variation from narrow gapped (< 20 meV) states [5] to rather pronounced DP band gap [1].

In the AFM phase (b) edges of the TSS are more pronounced than in the case within the PM phase (a). This has significant effect on the precision of the band gap estimation. The spectrum at T = 10 K ((g) blue curves) in the vicinity of the DP can be decomposed with two clearly separated peaks (solid blue) which reveal a gap size of 60 meV. However, at elevated temperatures (T = 35 K; (g) red curves) the peak decomposition is rather ambiguous and can be influenced by either of the following: a closing of the gap or a broadening of the peaks. The current fit returns a reduction of the DP gap by roughly 15 meV.

The most pronounce modification is significant drop of peaks' intensity drops between T = 10 K and T = 35 K. To track the intensity evolution between these two points we made temperature dependent analysis of the total spectral weight of the TSS near the DP by integrating intensity of spectra E(k) at each temperature point. Resulting dependence of the TSS intensity on the temperature is shown with blue triangles in (f). The TSS intensity of the AFM phase at T = 10 K is ~ 60 % larger than in the PM state. This points to significant change in the TSS upon the AFM/PM transition. The value of the (A)-state exchange splitting is added in (f). One can see that both dependencies well match each other regarding onset temperature T_0 and overall behavior. Therefore, the TSS intensity also seems to be dominated by the power law dependence on temperature as the exchange splitting of peak (A). From these facts we can establish that the Dirac cone spectral weight is influenced by the presence of the AFM phase. This finding could be a very important result since it may be the direct evidence for an interaction between the Dirac cone states and magnetic phase in the MBT system.

REFERENCES

1. M. M. Otrokov, I. I. Klimovskikh, H. Bentmann, D. Estyunin et al., Nature 576, 416 (2019).
2. J.-Q. Yan, Q. Zhang, T. Heitmann, Z. Huang et al., Phys. Rev. Materials 3, 064202 (2019).
3. A. Zeugner, F. Nietschke, A. U. B. Wolter, S. Gass et al., Chem. Mater. 31, 2795 (2019).
4. D. A. Estyunin, I.I. Klimovskikh, A. M. Shikin, E.F. Schwier et al., APL Materials 8, 021105 (2020)
5. Y.-J. Hao, P. Liu, Y. Feng, X.-M. Ma et al., Phys. Rev. X 9, 041038 (2019).

Study of the Dirac point energy gap in various magnetically doped topological insulators

D. A. Estyunin[a], A.M. Shikin[a], A.A. Rybkina[a], I.I. Klimovskikh[a], A. Kimura[b], S. Kumar[c] and E.F. Schwier[c]

[a] *Saint Petersburg State University, Saint Petersburg, 198504 Russia*
[b] *Department of Physical Sciences, Graduate School of Science, Hiroshima, Japan*
[c] *Hiroshima Synchrotron Radiation Center, Hiroshima University, Hiroshima, Japan*

Keywords: topological insulator, the Dirac cone, magnetic doping, magnetic topological insulator

Magnetically-doped topological insulators (TI) are experimentally proved to host Quantum Anomalous Hall (QAH) effect [1,2]. Precise tuning of Cr-doped TI stoichiometry and concentration of magnetic dopant increased temperature of transition to QAH state up to 1 K [3]. Doping with other magnetic elements instead of Cr may lead to the even higher transition temperatures. For example, Gd atom possesses one of the highest

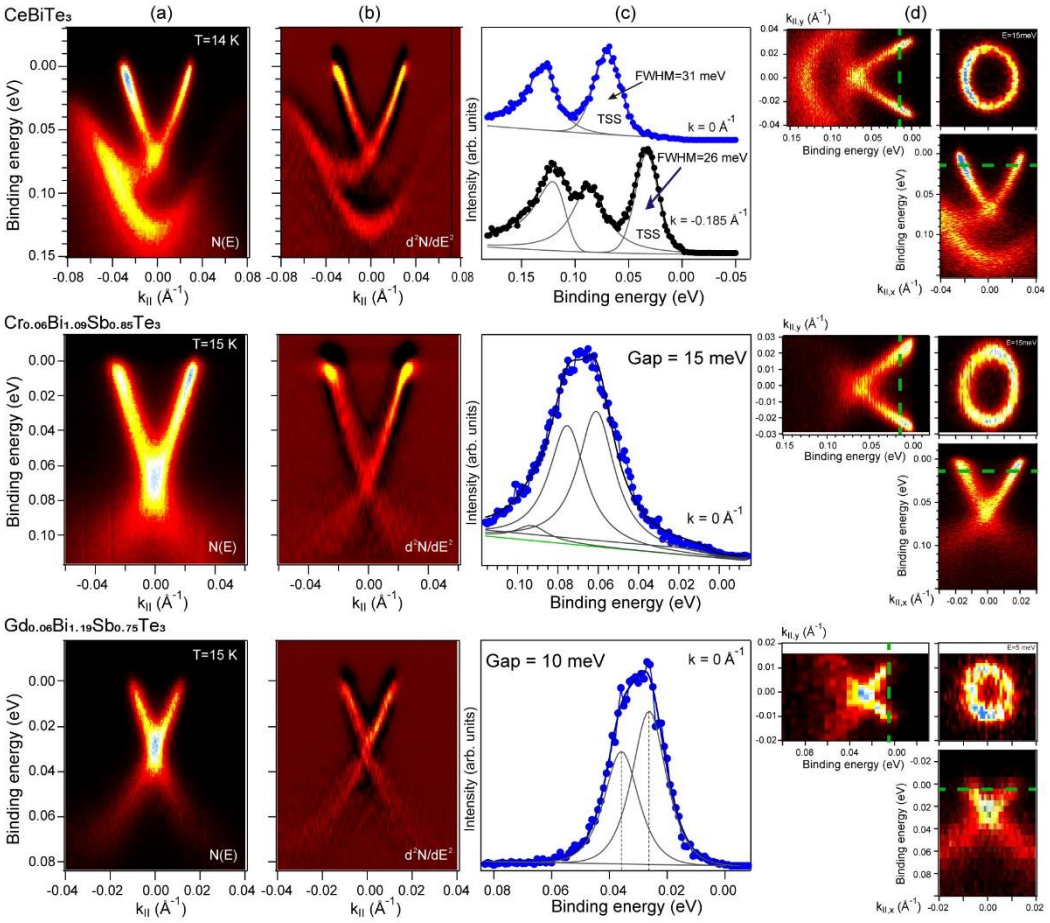

FIGURE 1. Experimental measured electronic structures with corresponding treatment of magnetically-doped TIs $CeBiTe_3$, $Cr_{0.06}Bi_{1.09}Sb_{0.85}Te_3$ and $Gd_{0.06}Bi_{1.19}Sb_{0.75}Te_3$. Measurements were acquired using laser radiation with hv = 6.3 eV at T= 14 - 15 K. For each sample panels (a) show dispersion relation as measured N(E), (b) – the second derivative d^2N/dE^2, (c) – energy distribution curves with corresponding spectral decompositions, (d) – mappings $E(k_{IIx}, k_{IIy})$ presented as cuts at constant energy (middle), along k_{IIx} at $k_{IIy} = 0$ Å^{-1} (bottom) and vice versa (left). Position of the constant energy cut is marked by green dashed line.

magnetic moments of ~ 8 μB and also can substituted Bi without electron (hole) transfer [4]. Other dopant we will present in this study is Ce which, though have lower magnetic moment, can possibly reach higher solubility in TI structure. The transition temperature refers to a size of the Dirac point band gap [5] which allows to estimated efficiency of the QAH state transition for each TI by means angular resolved photoemission spectroscopy (ARPES).

In this report we will present study of three magnetically doped TIs with stoichiometries $CeBiTe_3$, $Cr_{0.06}Bi_{1.09}Sb_{0.85}Te_3$ and $Gd_{0.06}Bi_{1.19}Sb_{0.75}Te_3$. For each sample we preliminary measured mapping $E(k_{IIx}, k_{IIy})$ to precisely distinguish position of the Γ-point (panels (d)). Any misalignment can cause a significant error in the estimation of the Dirac point gap size [6]. Dispersion relations for all three samples (see panels (a)) demonstrate pronounce Dirac cone state with some variation in shape from one compound to another. One can see that the position of the Dirac point (in binding energy) decreases from ~70 meV for $CeBiTe_3$ and Cr-doped TI to ~30 meV for Gd-doped TI. Difference in the Dirac point positions might relate to the amounts of Sb and magnetic impurities in TIs or/and maybe caused by irradiation induced band bending [7]. Moreover, in case of $CeBiTe_3$ valance band states are clear visible below the Dirac cone state.

The Dirac point gap is hardly distinguishable from as measured spectra and their second derivative (see panels (b)). Therefore, for more precise and quantitative analysis we give attention to the energy distribution curves at the Γ-point (panels (c)). We made corresponding decompositions with several Voight peaks to fit experimental data (shown with blue/black dots). One can see that in case of Cr- and Gd-doped TI decomposition requires two peaks for the Dirac cone state i.e. upper and lower parts of the Dirac cone are separated. Estimations yield the gap size of about 15 meV for Cr-doped and about 10 meV for Gd-doped. Note that peaks parameters for the decomposition were taken from the profiles away the Γ-point, where both peaks are well resolved, and extrapolated to the Γ-point. The Dirac cone state in case of $CeBiTe_3$ can be well fitted with one peak. Moreover, its full width at half maximum (see panel (c) for this compound) is almost constant moving away from the Γ-point to k_{II}= -0.185 $Å^{-1}$. At least we can assume that the gap size is less than 5 meV. In total, dispersion relation for $CeBiTe_3$ is reminiscent of the one for pure Bi_2Te_3.

Overall, we did not reach significant increasement of the gap size using Ce and Gd atoms for doping $(Bi,Sb)_2Te_3$ TI in comparison with Cr-doped TIs. Probably, $CeBiTe_3$ in our experiments had much lower concentration of Ce as was expected which resulted to the same electronic structure as in pure TI. Despite higher magnetic moment of Gd, it leads to smaller Dirac point band gap than Cr with equal concentration of dopants. This may be caused by difference in f and d magnetism.

REFERENCES

1. C.-Z. Chang, J. Zhang, X. Feng et al., Science 340, 167 (2013)
2. Y. Tokura, K. Yasuda, and A. Tsukazaki, Nat. Rev. Phys. 1, 126 (2019)
3. M. Mogi, R. Yoshimi, A. Tsukazaki et al., Appl. Phys. Lett. 107, 182401 (2015)
4. A. M. Shikin, D. A. Estyunin, Y. I. Surnin et al., Sci. Rep. 9, 4813 (2019)
5. C.-Z. Chang and M. Li, J. Phys.: Condens. Matter 28, 123002 (2016)
6. A. M. Shikin, A. A. Rybkina, D. A. Estyunin et al., Phys. Rev. B 97, 245407 (2018)
7. E. Frantzeskakis, S. V. Ramankutty, N. de Jong et al., Phys. Rev. X 7, 041041 (2017)

ARPES Studies of the Polarization-Dependent Features of the Electronic Structure of Ultrathin Ferromagnetic Films Grown on the PST and BSTS Topological Insulators for Spintronic Applications

Andrey K. Kaveev,[a] Oleg E. Tereshchenko,[b] Vladimir A. Golyashov[b] and Eike F. Schwier[c]

[a]*Ioffe Institute, 194021, 26 Polytechnicheskaya str., Saint-Petersburg, Russia*
[b]*Rzhanov Institute of Semiconductor Physics, 630090, 13 Ac. Lavrentev av., Novosibirsk, Russia*
[c]*Hiroshima University, 739-8527, Higashi Hiroshima, Japan*

Keywords: Topological insulators, PbSnTe, $BiSbTeSe_2$, Dirac cone, ferromagnetic metal, interface.

The control of the spectrum of surface topological states of topological insulators is attractive from the point of view of possible applications in spintronics. In particular, the influence of the proximity effect when depositing or introducing a magnetic impurity into the surface layer can remove the topological protection of states by removing the inversion with respect to time reversal symmetry [1]. Here we continue the studies began in HiSOR at 2017. Co was deposited on the $BiSbTeSe_2$(0001) surface with use of molecular beam epitaxy method. $BiSbTeSe_2$ mono-crystalline substrates were made from bulk monocrystals grown by the modified vertical Bridgeman method from the previously synthesized mixture of 5N pure Bi, Sb, Te and Se. Clean TI surfaces were obtained by the cleaving with a scotch tape and a subsequent vacuum annealing at 330°C under the 10^{-8} mBar pressure. Co atoms were deposited on the substrate at 330°C in vacuum. The effective thicknesses were between 0 and 2 Å. It should be taken into account that there are sub-monolayer coverages. The electronic structure of the grown samples was studied by laser based microfocused angle-resolved photoelectron spectroscopy (laser-ARPES, p-polarization).

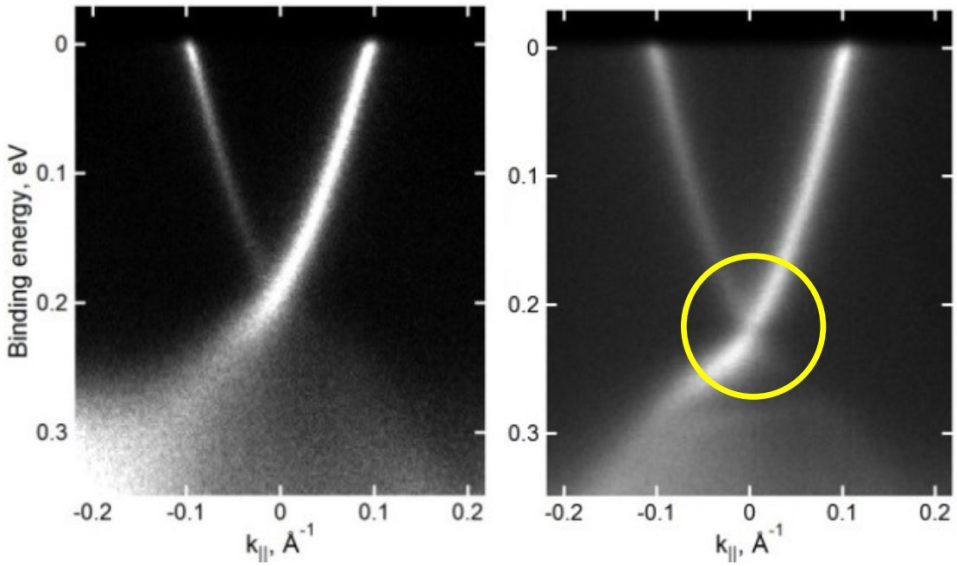

FIGURE 1. The result of bending of the surface bands after deposition of 0.1 Å of Co adsorbate at room temperature (Dirac point is observed) (a) and the band gap opening (b) in the spectrum of Dirac surface states in the Co / $BiSbTeSe_2$ system. Figure (b) corresponds to the deposition of 0.6 Å of Co at 300 °C.

The effect of the displacement of the Dirac point due to the band bending downwards (electron doping) was revealed using cobalt as adsorbate deposited at room temperature. This band bending leads to a shift of the Dirac point below the Fermi level, which made it possible to observe the region near the Dirac point by ARPES (Fig. 1). The energy gap width was estimated as 15–25 meV. Temperature measurements above 15 K showed the stability of the band gap to an increase in temperature. A mechanism is known for the formation of a gap of a nonmagnetic nature, which can be associated with the hybridization of surface states from two opposite surfaces of a topological insulator arising from the penetration of metal atoms into the van der Waals gaps between the atomic quintiles of topological insulators based on chalcogenides and that destroy the van der Waals bond [2]. However, in our case, this mechanism is not applicable because of the small amount of precipitated substance (less than one monolayer), which is not sufficient for diffusion through at least 4-5 quintuple-layers of the substrate to open a gap of similar width (~ 50 meV in [2]). Thus, we can make an assumption about the magnetic nature of the gap.

The studies of the band structure of PST with deposited ferromagnetic atoms are underway. The work was supported by the RFBR grant № 18-29-12094.

REFERENCES

1. X.-L. Qi, T.L. Hughes and S.-C. Zhang, *Phys. Rev. B*, 78, 195424, (2008).
2. Y. Zhang et al., *Nat. Phys*. 6, 584–588, (2010).

Micro-ARPES study of topological material Ag-doped Bi_2Se_3

Ritsuko Eguchi[a], Eike F. Schwier[b], Lei Zhi[a], Tomoya Taguchi[a], Kaya Kobayashi[a], Hidenori Goto[a], and Yoshihiro Kubozono[a]

[a]*Research Institute for Interdisciplinary Science, Okayama University, Okayama 700-8530, Japan*
[b]*Hiroshima Synchrotron Radiation Center, Hiroshima University, Higashi-Hiroshima 739-0047, Japan*

Keywords: Topological insulator, Ag-doped Bi_2Se_3, Laser-ARPES

Bi_2Se_3 is a typical topological insulator which is characterized by an insulating bulk state and a metallic surface state. When doped with impurity atoms, Bi_2Se_3 exhibits various ordered phenomena such as superconductivity and ferromagnetism [1-7]. We found that ultrathin crystals of Ag-doped Bi_2Se_3 showed semiconductor-metal (S-M) transition; resistance increased with decreasing temperature, while it abruptly decreased below the critical temperature, T_{cr} = 35 K [8]. Hall effect measurements indicated that decrease in resistance below T_{cr} was accompanied by decrease in electron density and mobility. Furthermore, measurement of the electric-field effect showed that the Fermi level was pinned at the bottom of the bulk conduction band (BCB) above T_{cr}, and it was raised into the BCB below T_{cr}. However, no structural phase transition and no meaningful change in lattice constants were observed at T_{cr} from single-crystal X-ray diffraction. Therefore, the presence of a novel electronic transition is expected to occur in ultrathin crystals of Ag-doped Bi_2Se_3.

The purpose of this study is to verify the temperature dependence of the Fermi level suggested by the transport measurement. The S-M transition was not observed in bulk crystals but in ultrathin crystals (typical size is several tens of μm and thickness around 100 nm). The observation with Micro-angle resolved photoelectron spectroscopy (ARPES) is indispensable to study the band structure and the Fermi level in such small crystals. In this experiment, firstly, we measured the temperature dependence of ARPES for flakes of Ag-doped Bi_2Se_3.

Micro-ARPES measurements were performed using Laser-ARPES apparatus in HiSOR. The laser of 197 nm (6.34 eV) in wavelength was used to excite photoelectrons. We prepared the flakes of non-doped and Ag-doped Bi_2Se_3 crystals to compare their electronic structures. These crystals were cleaved in an ultrahigh vacuum of 1.1×10^{-9} Pa at room temperature. The ARPES data was taken at 14 and 60 K.

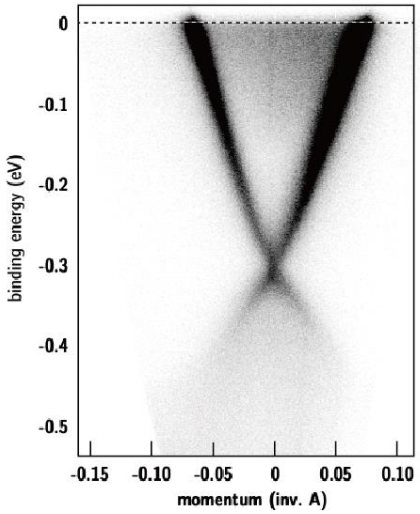

FIGURE 1. Band dispersion of $Ag_{0.1}Bi_2Se_3$ measured at 14 K.

Figure 1 shows the image plot of the band dispersion of $Ag_{0.1}Bi_2Se_3$ measured at 14 K. A clear Dirac cone of the surface states was observed. The Dirac point is recognized at the Γ point and is located at a binding energy of ~ 0.3 eV with a sizable gap of 35-40 meV. We tried to measure the temperature dependence of ARPES of $Ag_{0.1}Bi_2Se_3$. However, no remarkable change was observed in the electronic structure above and below T_{cr}. We found inhomogeneous electronic structure in the crystalline surface of Ag-doped Bi_2Se_3. Therefore, further experiments will be required to confirm the reproducibility of the gap opening and to conclude whether the temperature dependence of the electronic structure is observed or not. Additionally, we will try to measure ARPES of ultrathin crystals of Ag-doped Bi_2Se_3.

REFERENCES

1. Y. S. Hor, J. G. Checkelsky, D. Qu, N. P. Ong, and R. J. Cava, *J. Phys. Chem. Solids*. **72**, 572 (2011).
2. Z. Ren, A. A. Taskin, S. Sasaki, K. Segawa, and Y. Ando, *Phys. Rev. B* **84**, 075316 (2011).
3. M. Kriener, K. Segawa, Z. Ren, S. Sasaki, S. Wada, S. Kuwabata, and Y. Ando, *Phys. Rev. B* **84**, 54513 (2011).
4. Z. H. Liu *et al*., *J. Am.Chem.Soc*. **137**, 10512 (2015).
5. Y. S. Hor *et al*., *Physical Review B* **81**, 195203 (2010).
6. P. P. J. Haazen *et al*., *Appl. Phys. Lett*. **100**, 082404 (2012).
7. T. He *et al*., *Phys. Rev. B* **97**, 104503 (2018).
8. E. Uesugi *et al*., *Scientific Reports* **9**, 5376 (2019).

High Resolution Laser-ARPES Study on Magnetic Topological Insulators $MnBi_4Te_7$

Xiao-Ming Ma[a], Yu-Jie Hao[a], Yue Feng[a], Meng Zeng[a], Zhanyang Hao[a], Yuan Wang[a], Shiv Kumar[b], Eike F. Schwier[b], Kenya Shimada[b], Chaoyu Chen[a] and Chang Liu[a]

[a] *Shenzhen Institute for Quantum Science and Engineering (SIQSE) and Department of Physics, Southern University of Science and Technology (SUSTech), Shenzhen 518055, China.*
[b] *Hiroshima Synchrotron Radiation Center, Hiroshima University, Higashi-Hiroshima, Hiroshima 739-0046, Japan*

Keywords: Magnetic Topological Insulator, $MnBi_6Te_{10}$, Angle Resolved Photoelectron Spectroscopy.

The recent reported intrinsic magnetic topological insulator $MnBi_2Te_4$ have been met with unusual success in hosting exotic phenomena such as the quantum anomalous Hall effect and the axion insulator states [1-6]. Actually, the $MnBi_2Te_4$ is one number of the intrinsic topological insulators Mn-Bi-Te family. The compounds of the Mn-Bi-Te family compose the superlattice-like $MnBi_2Te_4/(Bi_2Te_3)_n$ (n = 0, 1, 2, 3…) layered structure, remains intriguing but elusive[7,8]. We systematically performed electronic band structure measurements on $MnBi_4Te_7$ by the high-resolution LASER angle resolved photoelectron spectroscopy (ARPES) at HiSOR.

Single crystal of $MnBi_4Te_7$ was grown out by flux method and the crystallinity was examined by X-ray diffraction (XRD). As shown in Fig. 1 (b), all peaks in the XRD pattern of the $MnBi_4Te_7$ powder can be well indexed by the calculated results with a space group of P - 3 m1 with $a = b$ = 4.355 Å, c = 23.815 Å. As shown in Fig. 1 (a), the lattice of $MnBi_4Te_7$ consists of one septuple $MnBi_2Te_4$ layer (SL) and one quintuple Bi_2Te_3 layers (QL) alternately stacking along the c axis [Fig.1 (a)]. These SLs or QLs are coupled through weak van der Waals forces. Cleaving the single crystal perpendicular to the c axis could have two possible terminations, i.e., S-termination and Q-termination.

The temperature dependence of magnetization measurement [Fig. 1(c)] establishes a long-range AFM order below Nèel temperature, T_N = 12.5 K. A sharp cusp around T_N for H//c, in contrast to the saturating plateau for H//ab, suggests that the magnetization-easy axis is the c direction. All these behaviors are consistent with an A-type AFM configuration (intralayer FM and interlayer AFM) along c-axis.

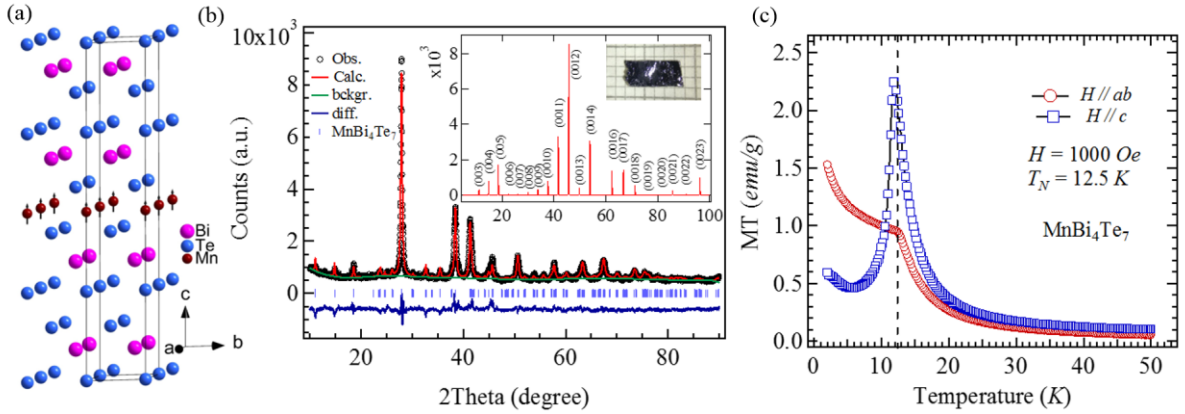

FIGURE 1. Crystal structure and magnetic properties of $MnBi_4Te_7$. (a) Schematic diagram of crystal structure of $MnBi_4Te_7$. (b) Powder X-ray diffraction data and the refinement calculated result. Inset: XRD results of the $MnBi_4Te_7$ single crystal and image of one piece crystal on top of a millimeter grid. (c) Temperature dependence of magnetization measured at applied field H = 0.1 T for H // ab (red circle) and H // c (blue square).

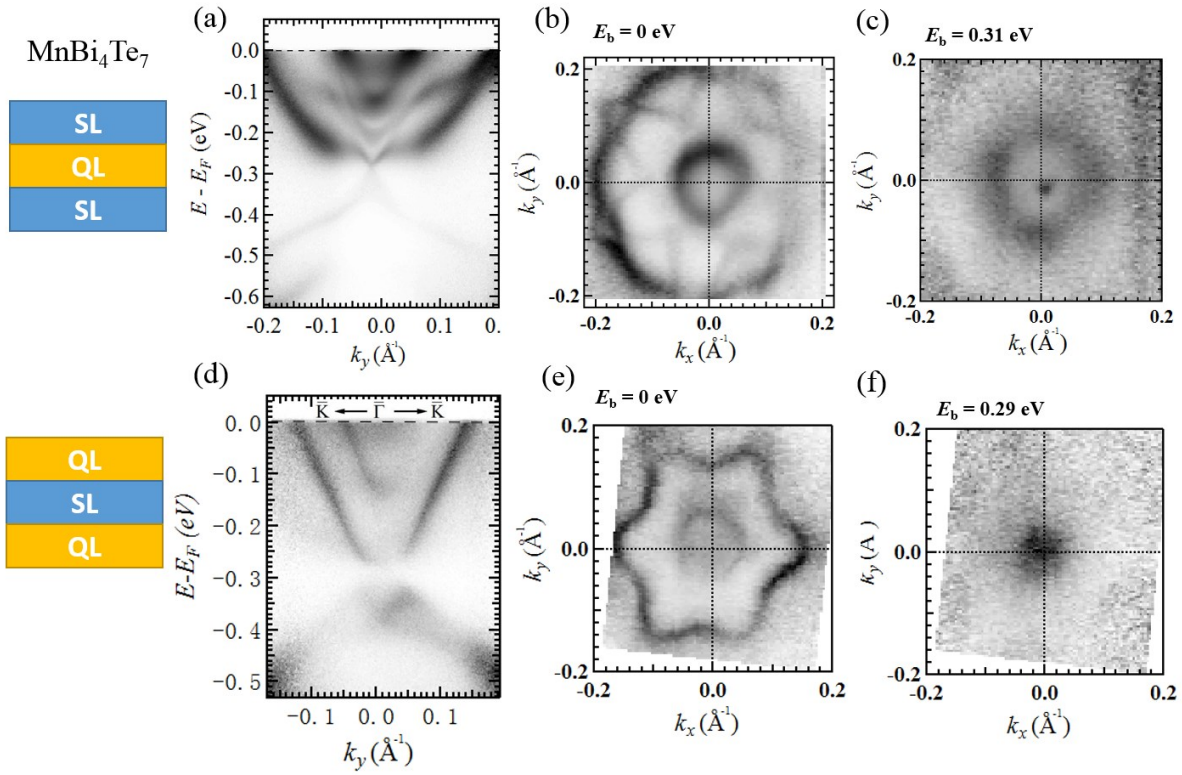

FIGURE 2. Termination-dependent electronic structure of $MnBi_4Te_7$. (a) Band dispersion along the high symmetry direction of S-termination. (b) and (d) are the constant energy contours results with indicated E_b. (d)-(f) are the similar results to (a)-(c) but for Q- termination.

The ARPES spectra for the two intrinsic terminations (S-and Q-terminations) of the $MnBi_4Te_7$ are presented in Figure 2. The constant energy contours with indicated E_b and the dispersions along high symmetry direction are given. The band disperson of the S-termination presents a galss shap band and there is very conspicuous Dirac crossing band can be observed [Figure 2 (a)]. For the Q-temination, an apparent gapped band sturcure dispersion was oberved [Figure 2 (d)]. It should be noted taht we were not able to observe the difference of the topological surface states above and below T_N.

We have put the article about these ARPES results and some further scanning tunneling microscope measurements on arxiv.org, and more detailed data and analysis can be found in Ref. [9].

REFERENCES

1 Y. Tokura, K. Yasuda, and A. Tsukazaki, Magnetic Topological Insulators, Nat. Rev. Phys. **1**, 126 (2019).

2 C.-Z. Chang et al., Experimental Observation of the Quantum Anomalous Hall Effect in a Magnetic Topological Insulator, Science **340**, 167 (2013).

3 R. Yu, W. Zhang, H.-J. Zhang, S.-C. Zhang, X. Dai, and Z. Fang, Quantized Anomalous Hall Effect in Magnetic Topological Insulators, Science **329**, 61 (2010).

4 Y. Gong et al., Experimental Realization of an Intrinsic Magnetic Topological Insulator, Chin. Phys. Lett. **36**, 076801 (2019).

5 J.-H. Li, Y. Li, S. Du, Z. Wang, B.-L. Gu, S.-C. Zhang, K. He, W. Duan, and Y. Xu, Intrinsic Magnetic Topological Insulators in van der Waals Layered $MnBi_2Te_4$-Family Materials, Sci. Adv. **5**, eaaw5685 (2019).

6 D. Zhang, M. Shi, T. Zhu, D. Xing, H. Zhang, and J. Wang, Topological Axion States in the Magnetic Insulator $MnBi_2Te_4$ with the Quantized Magnetoelectric Effect, Phys. Rev. Lett. **122**, 206401 (2019).

7 J.-Q. Yan, Y. H. Liu, D. Parker, M. A. McGuire, and B. C. Sales, A-type Antiferromagnetic order in $MnBi_4Te_7$ and $MnBi_6Te_{10}$ single crystals, arXiv:1910.06273 (2019).....

8 C. Hu et al., Realization of an intrinsic, ferromagnetic axion insulator in $MnBi_8Te_{13}$, arXiv:1910.12847.

9 Xuefeng Wu, et al. Distinct Topological Surface States on the Two Terminations of $MnBi_4Te_7$. arXiv:2002.00320 (2020).

ARPES Study on In-plane Antiferromagnetic Axion Insulator Candidate $EuIn_2As_2$

Yang Zhang[a], Ke Deng[b], Xiao Zhang[a], Meng Wang[a], Yuan Wang, Cai Liu[a], Jia-Wei Mei[b], Shiv Kumar[c], Eike F. Schwier[c], Kenya Shimada[c], Chaoyu Chen[b] and Bing Shen[a]

[a]*School of Physics, Sun Yat-Sen University, Guangzhou, Guangdong 510275, China*
[b]*Shenzhen Institute for Quantum Science and Engineering (SIQSE), Southern University of Science and Technology, Shenzhen 518055, China*
[c]*Hiroshima Synchrotron Radiation Center, Hiroshima University, Higashihiroshima, Hiroshima 739-0046, Japan*

Keywords: axion insulator, $EuIn_2As_2$, antiferromagnetic order (AFM order), hole pocket, ARPES

Topological materials intertwined with magnetism can lead to novel physics such as quantum anomalous Hall effect (QAHE) [1-3] and axion electrodynamics [4-7]. However. it is experimentally challenging to achieve the coexistence of intrinsic magnetic order and topological nontriviality. To date, layered structural compound $MnBi_2Te_4$ is the first established TI with intrinsic magnetic order [8-14], although half quantized conducting plateau and Chern-axion insulator transition have been observed in few layers of $MnBi_2Te_4$ [15-17], subsequent ARPES experiment on bulk crystal of $MnBi_2Te_4$ revealed unexpected gapless surface state [18-21], which suggesting the cleaved surface might suffer from a destroyed surface magnetic configuration and is hard to achieve axion insulator states in its bulk crystal. Observing the gapped topological surface state is therefore crucial for realizing the anxion insulator states.

Different from the magnetic TI $MnBi_2Te_4$ with van der Waals layered structure, $EuIn_2As_2$, exhibit a three-dimensional structure and antiferromagnetic order is proposed for realizing both axion insulator and high order topological insulator states thanks to its interplay of magnetism and nontrivial topology which can be effectively described by theta term as below [22].

$$S_\theta = \frac{\theta e^2}{4\pi^2}\int dt \cdot d^3\boldsymbol{x}\boldsymbol{E}\cdot\boldsymbol{B}$$

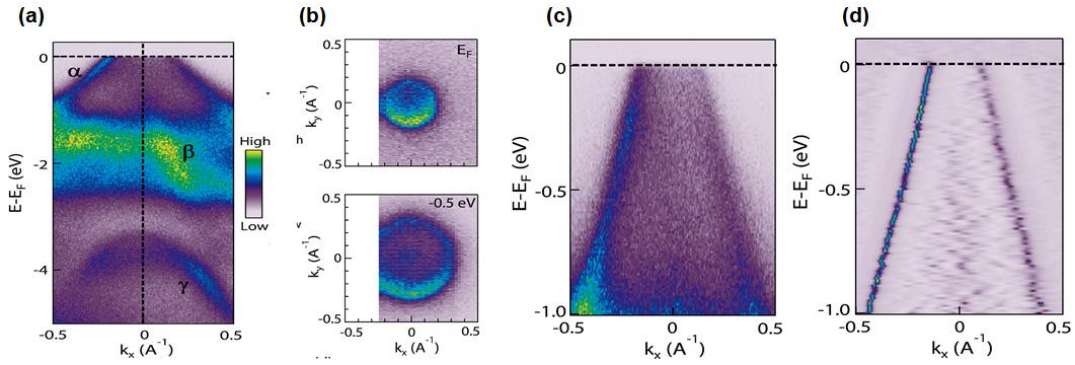

FIGURE 1. Our previous ARPES data of pristine $EuIn_2As_2$ crystal: (a)Valence band structure along the K-Γ-K direction (b) Fermi surface map (top) and constant energy contour at -0.5 eV below E_F (down) (c) Zoom-in of the valence band in (a). (d) 2nd derivative EDCs of (c) to highlight the hole band dispersion [23].

Our recent ARPES measurement of pristine $EuIn_2As_2$ crystal (Fig. 1) show a linear hole-type dispersion

dominates the electron dispersions around E_F. In total there are 3 valence bands (from low to high banding energy) near Fermi level were observed along the K-Γ-K direction of Brillouin zone (Fig. 1 (a)). According to the theoretical calculation [22], 5*s* and 4*p* orbits of In and As respectively dominate the dispersion features near E_F. And all the important dispersions reside around Γ point. We therefore focus on the certain momentum window around Γ point as shown in Fig. 1(a). A circular hole-like pocket grows in sizes with increasing binding energy agrees well with Fig. 1(a), and carrier density of pristine $EuIn_2As_2$ can be calculated as $2.2 \times 10^{13}\ cm^{-2}$ according to Luttinger theorem with single band contribution. A zoom-in of Fig. 1(a) enables us to scrutinize the dispersion of the surface band and fit the energy dispersion $E(k)$ using momentum distribution curve (MDC) cuts. The extracted $E(k)$ curve is linear with Fermi velocity of $3.7\ eV \cdot A$ $(5.7105\ m/s)$ and $k_F = 0.12\ \text{Å}^{-1}$ (Fig. 1(c) and (d)). In addition, we note that by using the extracted k_F and Fermi velocity, the topmost of the hole pocket can be estimated as about 300 meV above E_F in which resides the topological surface state according to calculation [22]. In consistancy with our transport measurements [23], the ARPES measurements indicate the pristine $EuIn_2As_2$ is in metallic state rather than an insulator with E_F lies in gap. Further tuning the chemical potential by doping or gating electron would lift the Fermi level close to the predicted topological surface state.

REFERENCES

1. F. D. M. Haldane, Phys. Rev. Lett. 61, 2015 (1988).
2. Rui Yu, et al., Science 329, 61 (2010)..
3. Cui-Zu Chang, et al.,Science 340, 167 (2013).
4. R Li, et al. Nat. Phys., 2010, 6(4): 284.
5. X. L. Qi and S-C Zhang, Rev. Mod. Phys. 83, 1057 (2011).
6. N. P. Armitage and Liang Wu, Sci. Post. Phys. 6, 046 (2019).
7. Di Xiao, et al., Phys. Rev. Lett. 120, 056801 (2018).
8. M. M. Otrokov, et al., Nature 576, 416 (2019).
9. Roger S. K. et al., Nature 576, 390 (2019).
10. E. D. L. Rienks, et al., Nature 576, 423 (2019).
11. M. M. Otrokov, et al., Phys. Rev. Lett. 122, 107202 (2019).
12. J. Li, et al. Sci. Adv. 5, eaaw5685 (2019).
13. J. Li, et al., Phys. Rev. B 100, 121103(R) (2019).
14. D. Zhang, et al., Phys. Rev. Lett. 122, 206401 (2019).
15. Y. Deng, et al., science 367, 895 (2020).
16. C. Liu, et al., Nat. Mater. 19, 522–527(2020)
17. Jun Ge, et al., Nat. Sci. Rev., nwaa089, https://doi.org/10.1093/nsr/nwaa089.
18. Y. Hao, et al., Phys. Rev. X 9, 041038 (2019).
19. Y. J. Chen, et al., Phys. Rev. X 9, 041040, (2019)
20. H. Li, et al., Phys. Rev. X 9, 041039 (2019).
21. P. Swatek, et al., arXiv:1907.09596 (2019).
22. Y. Xu, et al., Phys. Rev. Lett. 122, 256402 (2019).
23. Y. Zhang, et al., Phys. Rev. B.101.205126 (2020).

Electronic Band Structure Study on the Surfaces of Magnetic Topological Insulators $MnBi_6Te_{10}$

Xiao-Ming Ma[a], Zhongjia Chen[a], Eike F. Schwier[b], Yu-Jie Hao[a], Rui'e Lu[a], Yuanjun Jin[a], Meng Zeng[a], Xiang-Rui Liu[a], Zhanyang Hao[a], Ke Zhang[b], Wumiti Mansuer[b], Shiv Kumar[b], Yuan Wang[a], Cai Liu[a], Ke Deng[a], Jiawei Mei[a], Kenya Shimada[b], Wen Huang[a], Chang Liu[a], Hu Xu[a] and Chaoyu Chen[a]

[a] *Shenzhen Institute for Quantum Science and Engineering (SIQSE) and Department of Physics, Southern University of Science and Technology (SUSTech), Shenzhen 518055, China.*
[b] *Hiroshima Synchrotron Radiation Center, Hiroshima University, Higashi-Hiroshima, Hiroshima 739-0046, Japan*

Keywords: Magnetic Topological Insulator, $MnBi_6Te_{10}$, Angle Resolved Photoelectron Spectroscopy.

Recently, the antiferromagnetic $MnBi_2Te_4$ has arisen as the first magnetic topological insulator, hosting possible axion electrodynamics and quantum anomalous Hall effect in condensed matter [1-7]. In fact, $MnBi_2Te_4$ is one member of the ternary van der Waals compound series $(MnBi_2Te_4)_m(Bi_2Te_3)_n$ with [Te-Bi-Te-Mn-Te-Bi-Te] septuple (S) layers ([$MnBi_2Te_4$], SLs) and [Te-Bi-Te-Bi-Te] quintuple (Q) layers ([Bi_2Te_3], QLs) alternately stacking along the *c* axis [8,9]. While $MnBi_2Te_4$ has been extensively studied recently, its sister compounds with higher *n* number such as $MnBi_4Te_7$ (*n* = 1) and $MnBi_6Te_{10}$ (*n* = 2), remain less explored. We systematically performed electronic band structure measurements on $MnBi_6Te_{10}$ by the LASER angle resolved photoelectron spectroscopy (ARPES) at HiSOR.

$MnBi_6Te_{10}$ has a trigonal structure with a space group of R-3m with $a = b = 4.3745$ Å, $c = 101.985$ Å. The lattice of $MnBi_6Te_{10}$ consists of one septuple $MnBi_2Te_4$ layer and two quintuple Bi_2Te_3 layers alternately stacking along the *c* axis, as shown in Fig. 1 (a). These SLs or QLs are coupled through weak van der Waals forces. Cleaving the single crystal perpendicular to the *c* axis could have three possible terminations, i.e., S-termination, Q-termination and QQ-termination. The crystallinity was examined by X-ray diffraction (XRD). As shown in Fig. 1 (b), all peaks in the X-ray diffraction (XRD) pattern can be well indexed by the (00*l*) reflections of $MnBi_6Te_{10}$.

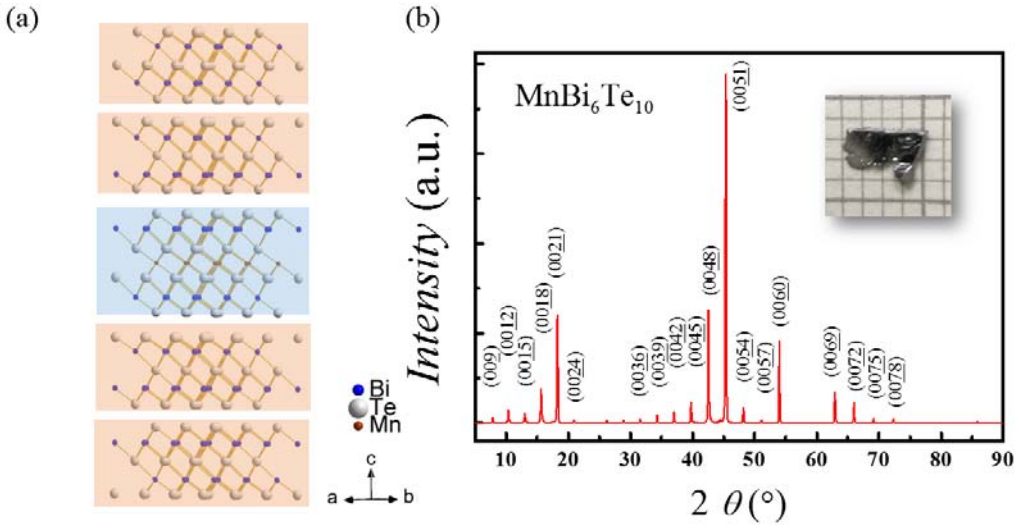

FIGURE 1. Crystal structure of $MnBi_6Te_{10}$. (a) The schematic lattice structure of $MnBi_6Te_{10}$ single crystals. (b) The single crystal XRD result and peak index result of $MnBi_6Te_{10}$. The inset is the picture of one piece of $MnBi_6Te_{10}$ single crystal.

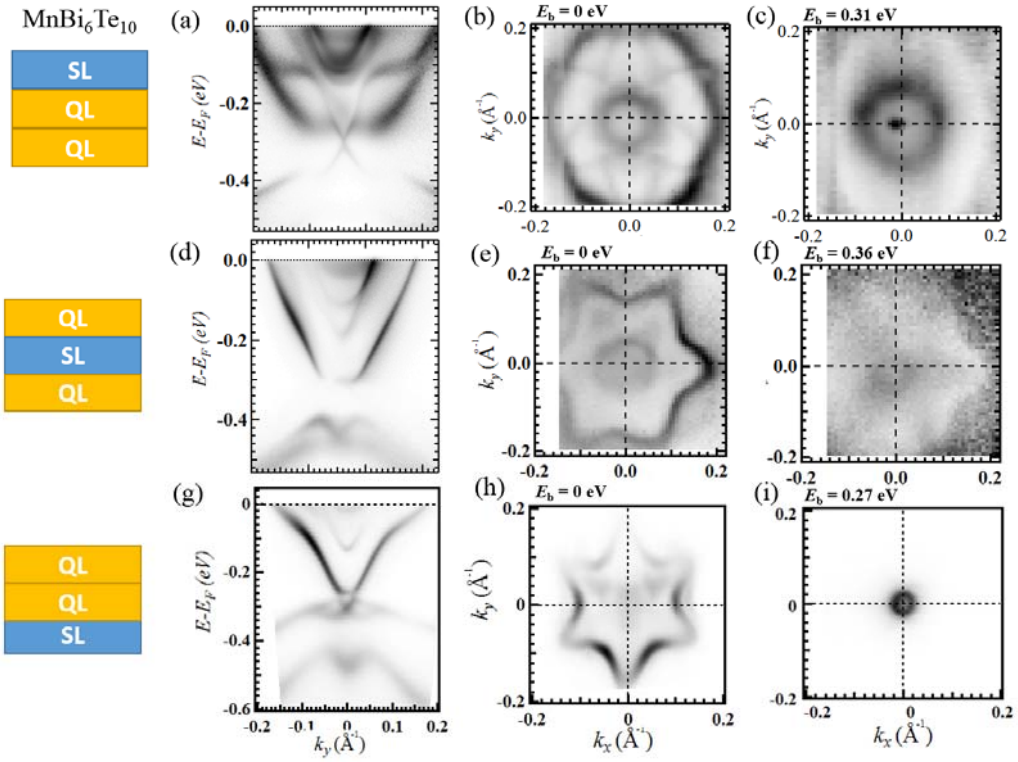

FIGURE 2. Termination-dependent electronic structure of $MnBi_6Te_{10}$. (a) Band dispersion along the high symmetry direction of S-termination. (b) and (d) are the constant energy contours results with indicated E_b. (d)-(f) and (g)-(i) are the similar results to (a)-(c) but for Q- and QQ-terminations, respectively.

The ARPES spectra for all the three intrinsic terminations (S-, Q- and QQ-terminations) of the $MnBi_6Te_{10}$ are presented in Fig. 2. The constant energy contours results with indicated E_b and the dispersion along high symmetry directions are given. From the size of the constant energy contours at the E_b = 0 eV, it is observed that the Fermi surfaces for the S-, Q- and QQ-terminations shrink gradually. A very conspicuous Dirac crossing band can be observed for the S-termination but the Q-temination presnts an apparent gapped band sturcure. For the QQ-termination, the band dispersion is more colese to Bi_2Te_3. The Néel temperature (T_N) of $MnBi_6Te_{10}$ is ~ 13 K, and this set ARPES data are collected above the T_N. We also did the measurement below the T_N, we can barely observed the difference caused by lower temperature.

We have written this ARPES result and further theoretical analysis into an article and more detailed experimental results and theoretical calculation can be found in Ref. [10].

REFERENCES

1 Mong, R. S. K. and Moore, J. E. Magnetic and topological order united in a crystal. Nature **576**, 390 (2019).
2 Otrokov, M. M. et al. Prediction and observation of an antiferromagnetic topological insulator. Nature **576**, 416 (2019).
3 Rienks, E. D. L. et al. Large magnetic gap at the Dirac point in Bi_2Te_3/$MnBi_2Te_4$ heterostructures. Nature **576**, 423 (2019).
4 Li, J. et al. Intrinsic magnetic topological insulators in van der Waals layered $MnBi_2Te_4$-family materials. Sci. Adv. **5**, eaaw5685 (2019).
5 Li, J. et al. Magnetically controllable topological quantum phase transitions in the antiferromagnetic topological insulator $MnBi_2Te_4$. Phys. Rev. B **100**, 121103 (2019).
6 Otrokov, M. M. et al. Unique Thickness-Dependent Properties of the van der Waals Interlayer Antiferromagnetic $MnBi_2Te_4$ Films. Phys. Rev. Lett. **122**, 107202 (2019).
7 Zhang, D. et al. Topological Axion States in the Magnetic Insulator MnBi2Te4 with the Quantized Magnetoelectric Effect. Phys. Rev. Lett. **122,** 206401 (2019).
8 Aliev, Z. S. et al. Novel ternary layered manganese bismuth tellurides of the MnTe-Bi_2Te_3 system: Synthesis and crystal structure. J Alloy Compd. **789**, 443 (2019).
9 Souchay, D. et al. Layered manganese bismuth tellurides with $GeBi_4Te_7$- and $GeBi_6Te_{10}$-type structures: towards multifunctional materials. J Mater. Chem. C **7**, 9939 (2019).
10 Xiao-Ming Ma et al. Hybridization-Induced Gapped and Gapless States on the Surfaces of Magnetic Topological Insulators. arXiv:1912.13237 (2019).

Instabilities and their competition in doped or intercalated VSe_2

C. S. Yadav[a], E. F. Schwier[b] and A. Taraphder[c]

[a] *School of Basic Sciences, Indian Institute of Technology Mandi, Kamand, Mandi-175005 (H.P.) India*
[b] *Hiroshima Synchrotron Radiation Research Center, Hiroshima University, Hiroshima-7390046 Japan*
c Department of Physics, Indian Institute of Technology Kharagpur, Kharagpur-721302 (W.B.) India

Keywords: Charge Density Wave, Angle-Resolved Photoemission Spectroscopy, Transition-Metal Dichalcogenides

VSe_2 is Group Vb TMDC and crystallizes in a trigonal prismatic structure, with unusually large c/a ratio of 1.82 in comparison to 1.633 for an ideal hexagonal system [1]. It has a CDW transition at 110 K, which is clearly visibly in electronic transport (resistivity, Hall, Seebeck coefficient) and magnetic properties [2]. Intercalation or doping of the magnetic element in the TMDCs gives rise to interesting properties. The TaS2 and NbSe2 shows a Kondo like minima upon 5% Fe intercalation. At 5 % Fe intercalation enhances the SC TC of TaS2 from 0.8 K to 3.3 K [3], while 25% Fe intercalation leads to the ferromagnetism below 160 K. [4] The band structure study on VSe2 suggests it to be an exchange enhanced paramagnet with a Stoner enhancement factor S ~ 4.5, [5] but FexVSe2system is shown to be non-magnetic at least up to 33% Fe intercalation [6]. Additionally, there is emergence of new transition at 160 K, with a broad hysteresis in electrical resistivity [6]. But the nature of this transition is still not clearly understood. It is suggested in the previous ARPES studies that CDW gap in VSe_2 is in fact a pseudo gap (Δ~ 80-100 meV) and consist of a finite density of states at Fermi level. This value of gap corresponds to $2\Delta/k_BT_C$ ~ 20, which is much larger than the mean field value (3.54) [7] indicating strong correlation.

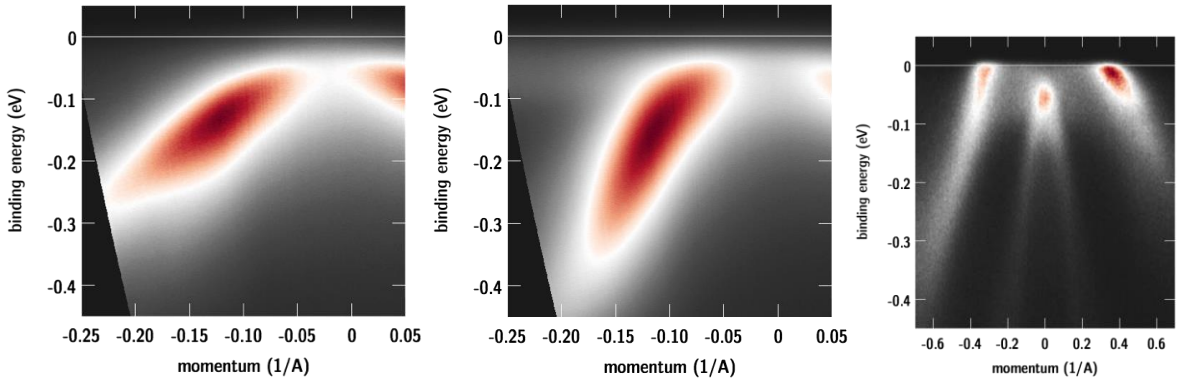

FIGURE 1. (left) VSe_2 Valence band at a temperature of 20 K. The measurement is within the s-polarization geometry along the GM high symmetry direction of the Surface Brillouin zone. The main contribution to the spectrum is supposed to be derived from the odd symmetry Se p_y orbital contribution to the electronic structure. The band maximum around the Γ-point is located around 60 meV below the Fermi level.
(middle) Same conditions as left, except the polarization vector of the light was rotated by $\pi/2$ and the measurement is performed in the p-pol geometry. Supposedly even states like Se p_x are the main contribution to the spectral weight. The weak non-dispersive band around a binding energy of 60 meV is visible and likely derived from the V *3d* bands, having weak cross-sections for photoexcitation at the energy of the Laser.
(right) VSe_2 Valence band at a temperature of 20 K and a photon energy of 50 eV within the p-polarization geometry of BL-1. Inversion of spectral weight depletion from the Laser energy is present in the Se derived hole bands around the Γ-point. The fral band however dues not increase in relative intensity.

With the final goal of controlling the phase transition of VSe_2 by means of 3d transition metal intercalation in mind, a detailed study of pristine VSe_2 single crystals was initially performed to function as a foundation of intercalation studies. Using ARPES, VSe_2 single crystals were investigated at the μ-Laser ARPES setup of the Hiroshima Synchrotron Radiation Center (HiSOR) [8]. In Figure 1 the valence bands of VSe_2 within its CDW phase (T = 20 K) are plotted along the GM high-symmetry direction of the surface Brillouin zone. Using s- (Figure 1, left) and p-polarized photons (Figure 1, middle), respectively.

In both spectra, bands of different symmetry within the Se *4p* manifold of the Valence band are expected to be excited based on the matrix element effects within the photoemission process. And indeed we find a heavy band to dominate the spectral weight of measurement using s-polarized photons and a light band in the p-polarization case. These can be regarded as representing anti-bonding and bonding states along the ΓM line respectively. Noteworthy is the depletion of spectral weight of the bands around the Γ-point. This effect is not due to the bands crossing the Fermi level, as the valence band maximum exhibits a binding energy of 60 meV. It is likely a hybridization effect of the V *3d* and Se *4p* states. This in turn should lead to vastly different cross-sections at the photon energy used by the Laser (hν =6.35 eV). As the calculated atomic cross-sections are 4 Mb for V *3d* and 30 Mb for Se *4p* [9], respectively.

Using a complementary photon energy of 50 eV at the end-station of the linear undulator beamline BL-1 at HiSOR [10] the atomic cross-sections calculate to 7 Mb for V *3d* and 0.3 Mb for Se *4p*. This would strongly favouring the excitation of the Vanadium states. Assuming the source of the depletion of spectral weight around the Γ-point is indeed the hybridization between V *3d* and Se *4p* orbitals, one would expect an inverted picture to the Laser measurement. The spectra obtained at this nominally V *3d* favourable energy (Figure 1, right) indeed shows the Se derived band around the Γ-point to exhibits now an inverted spectral weight distribution with the valence band maximum dominating the intensity and a depletion of spectral weight towards higher binding energies. Such hybridization of bands has been shown to exist in similar compounds like TiSe2 as well [11] and may be a key point in understanding the formation of the CDW phase.

At the same time, additional bands are crossing the Fermi level at $k_F \sim 0.3A^{-1}$. These are the well-known electron pockets who exhibit the pseudo-gap below the CDW transition temperature [12]. The node of the pseudo gap is along the ΓM direction which is why no gap is detected in the present spectra. There is however weak spectral weight seemingly connecting the electron pockets with the hole band around Γ. This intensity corresponds to the weak non-dispersive flat band observed in the Laser spectrum (Figure 1, middle) up to $0.25A^{-1}$. Weather it is part of the intrinsic band dispersion of VSe2 or a defect state is currently under investigation.

REFERENCES

1. C. F. Van Bruggen and C. Haas, *Sol. Stat. Comm.* **20**, 251 (1976).
2. C. S. Yadav and A. Rastogi, *Sol. Stat. Comm.* **150**, 648 (2010).
3. D. A. Whitney, R.M. Fleming and R. V. Coleman, *Phys. Rev. B* **15** 3405 (1977).
4. E. Morosan, H. W. Zandbergen, L. Li, M. Lee, et al., *Phys. Rev. B* **75** 104401 (2007).
5. H.W. Myron, *Physica B* **99** 243 (1980).
6. C .S. Yadav, and A.K. Rastogi, *J. Phys.: Cond. Matt.* **20**, 465219 (2008)
7. K. Terashima et al., *Phys. Rev. B* **68**, 155108 (2003).
8. H. Iwasawa and E. F. Schwier et al., *Ultramicroscopy, 182*, 85–91 (2017)
9. J. J. Jeh and I. Lindau, *Atomic Data and Nuclear Data Tables* 32 1-155 (1985)
10. H. Iwasawa and K. Shimada et al., *Journal of Synchrotron Radiation*, *24*(4), 836–841 (2017)
11. T. Jaouen et al. arxiv.org/abs/1911.06053 (2019)
12. J. Feng et al., *Nano Lett.* 2018, 18, 7, 4493–449 (2018)

Laser-photoemission spectroscopy on the magnetic topological insulators $V:(Bi,Sb)_2Te_3$ and $MnBi_2Te_4$

Philipp Kagerer, Raphael C. Vidal, Celso I. Fornari, Thiago R.F. Peixoto, Hendrik Bentmann and Friedrich Reinert

Experimental Physics VII
Physikalisches Institut
Universität Würzburg
Am Hubland
97074 Würzburg

Keywords: Topological insulators, magnetism, ARPES, high resolution, dichroism.

Starting from the first direct experimental observation of the topological surface states in Bi_2Se_3 [1] and related compounds by angle resolved photoemission spectroscopy (ARPES) the investigation of topological materials using photoemission techniques has become a very vivid research field. Especially the influence of magnetic order on the topological states remains an open question. While transport studies show sufficient evidence for a topological phase transition induced by the magnetic ordering to the quantum anomalous hall phase [2], the picture is still rather unclear, when directly imaging the surface state using ARPES. In the experiments conducted at the laser-based scanning µ-ARPES setup, we have investigated two classes of magnetic topological insulators. V-doped $(Bi,Sb)_2Te_3$, a material, for which the magnetic transition is already proven and well understood, and for which transport shows clear signatures of a quantized edge-state conductivity [3]. The second material class under investigation is the modular series of $(MnBi_2Te_4)(Bi_2Te_3)_n$, a novel topological nontrivial material, where the magnetism is intrinsically incorporated in the ordered crystalline structure [4-6].

The V-doped $(Bi,Sb)_2Te_3$ samples investigated in the experiments were MBE-grown thin films, grown by the group of Laurens Molenkamp, exp. Physics III, Univ. Würzburg. After growth, the samples were capped with a thick layer of Te to protect them against contamination and decapped in-situ in the measurement chamber at HiSOR. Using the highly focused Laser Source of the endstadtion and the strong control over the light polarization it was possible to resolve the topological surface state (TSS) dispersion in the band-gap of the material. The data is shown in fig. 1 for two different Bi, Sb ratios showing the very pronounced appearance of the upper branch of the TSS.

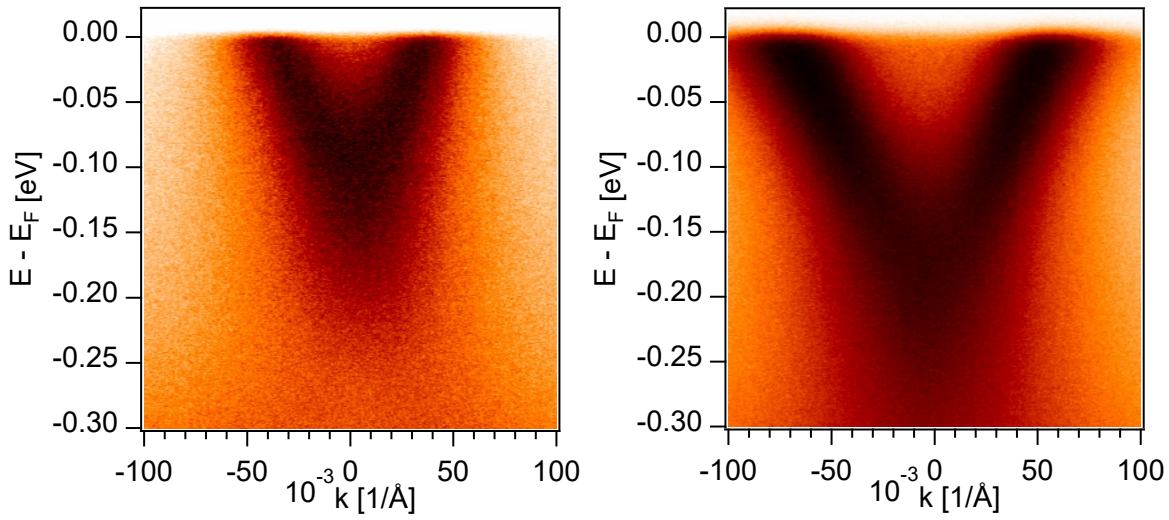

FIGURE 1. High resolution measurements of the topological surface state present in $V:(Bi,Sb)_2Te_3$ for different Bi/Sb ratios. The data clearly shows the appearance of the surface state in the material bandgap.

Utilizing the available polarizations and the very well-defined control over the sample temperature even below 10 K we were also able to study the temperature evolution of the TSS over the magnetic phase transition of the material. Polarization dependent measurements also hint towards the expected spin-polarization of the surface state as also known for the parent compound Bi_2Te_3 [7].

Furthermore, we investigated the electronic structure of the various surface terminations of $(MnBi_2Te_4)(Bi_2Te_3)_n$ for $n = 0,1,2$. The incorporation of non-magnetic Bi_2Te_3-layers strongly alters the electronic structure of the progenitor system $MnBi_2Te_4$. Due to the system consisting of stacked van der Walls layers, it is straightforward to access via exfoliation. For the compounds with $n > 0$ it is possible for the different terminations to occur on one sample. In order to unambiguously disentangle the electronic structure of occurring terminations, it is crucial to examine the system with light sources in the µm-range. The single crystals are provided by the group of M. Ruck [4].

Fig. 2 shows the surface electronic structure for the terminations of $(MnBi_2Te_4)(Bi_2Te_3)_n$, $n = 0,1,2$. There is a clear resemblance between the septuple-layer (SL) terminations of $MnBi_4Te_7$ and $MnBi_6Te_{10}$ as well as the quintuple-layer (QL) termination followed by a SL. Analogous to our $V:(Bi,Sb)_2Te_3$ study, we could utilize the temperature control in order to address the ongoing question of the magnetic gap in photoemission.

Additionally, we investigated the orbital character of the topological surface state by the means polarization dependent measurements. Circular dichroism unveils a spectral signature of the upper part of the Dirac state of SL termination of $MnBi_4Te_7$, which is not traceable by the bare photoemission intensity.

These and further experiments aid us to compliment the picture drawn in our previous publication [6].

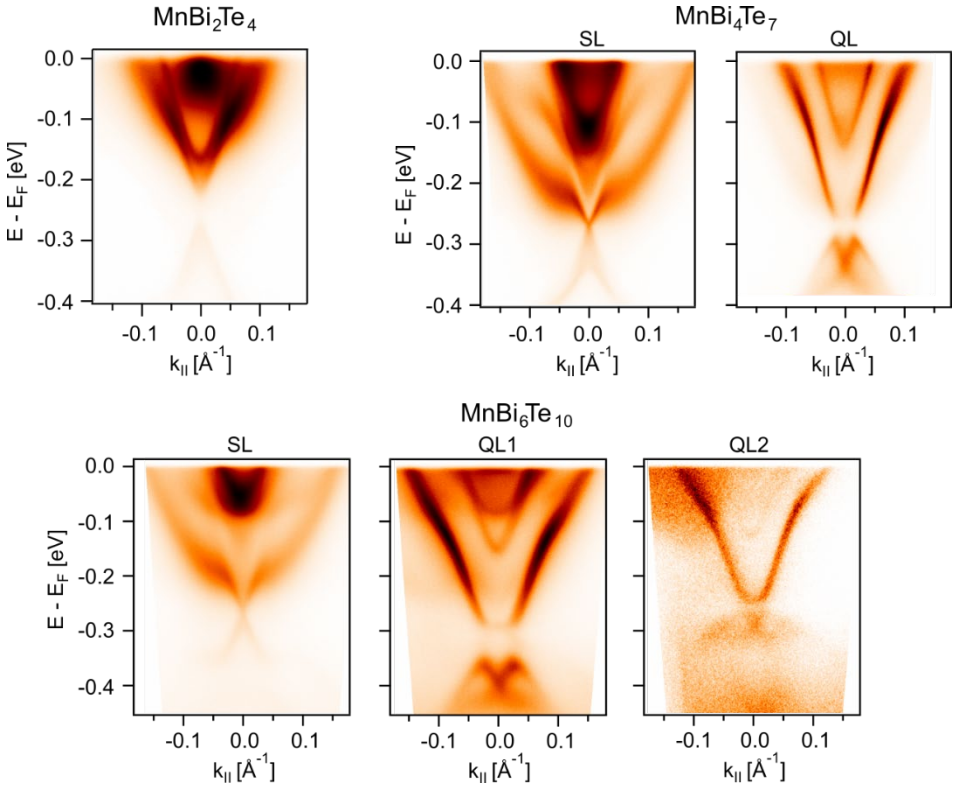

FIGURE 1. Surface electronic structure of all the occurring (0001) surface terminations of $(MnBi_2Te_4)(Bi_2Te_3)_n$ for $n = 0,1$ and 2. A close resemblance can be seen for the two terminations of $MnBi_4Te_7$ and the corresponding terminations of $MnBi_6Te_{10}$.

REFERENCES

1. H.Zhang et al., Topological insulators in . Bi_2Se_3, Bi_2Te_3 and $Sb_2Te_3$with a single Dirac cone on the surface, *nature physics* **5**, 438-442 (2009)
2. Transport paper, not on vbst

3. S.Grauer et al., Scaling of the Quantum Anomalous Hall Effedt as an Indicator on Axion Electrodynamics, *Phys. Rev. Lett*. **118**, 246801 (2017)
4. A.Zeugner et al., Chemical Aspects of the Candidate Antiferromagnetic Topological Insulator $MnBi_2Te_4$, *Chem.Mater.* **31**, 2795-2806 (2019)
5. R. C. Vidal, Surface states and Rashba-type spin polarization in antiferromagnetic $MnBi_2Te_4(0001)$, Phys. Rev. B **100**, 121104(R), 2019.
6. R. C. Vidal, Topological Electronic Structure and Intrinsic Magnetization in $MnBi_4Te_7$: A Bi_2Te_3 Derivative with a Periodic Mn Sublattice, Phys. Rev. X **9**, 041065 (2019)
7. C.Seibel, Photoelectron spin polarization in the $Bi_2Te_3(0001)$ topological insulator: Initial- and final-state effects in the photoemission process, *PhysRevB*. **93**, 245150 (2016)